DIAGNOSIS OF DIVERGENCE IN A THREE-PARAMETER NUMERICAL PREDICTION MODEL

A. WIIN-NIELSEN

Joint Numerical Weather Prediction Unit, Air Weather Service, Suitland, Md.
[Manuscript received November 9, 1960; revised January 11, 1961]

ABSTRACT

The equation for the vertical velocity in a quasi-non-divergent, three-parameter model has been solved for a certain simple flow pattern. The importance of vertical variation of static stability and of the horizontal wind is discussed from the solutions. Examples showing the distribution of divergence relative to the synoptic systems are computed and compared with those obtained by other investigators. A general discussion of the factors influencing the mid-tropospheric divergence follows in section 4, and section 5 contains finally some remarks on the divergence in very long waves.

1. INTRODUCTION

The distribution of convergence and divergence and of vertical velocity relative to the atmospheric flow pattern has been a very important and most intriguing problem in synoptic and dynamic meteorology for many years. Due to the fact that these quantities have to be obtained by indirect methods numerous rules relating the distribution of divergence to the synoptic flow pattern have been formulated. Intensive synoptic studies (Fleagle, [2]) have resulted in characteristic distributions of divergence relative to the troughs and ridges. Theoretical studies by Charney [1] and others using a very general continuous model gave as a by-product the divergence fields in baroclinic waves. General agreement between the results of the synoptic and theoretical studies was apparent.

The different dynamical models applied in numerical weather prediction and in studies of the general circulation, except the non-divergent model, contain implicitly distributions of divergence and vertical velocity, but because most of the time integrations have been made with one- or two-parameter models it has not been too interesting to study the predicted distributions since the vertical variations are constrained to very simple patterns like parabolic distributions of vertical velocity with pressure and linear variations of divergence.

The experiments with quasi-non-divergent two-parameter models have shown that these models are not sufficiently accurate to predict the developments of strong baroclinic nature. Several reasons may be mentioned for these somewhat discouraging results, but it is evident that the two-parameter model which assumes a constant direction of the thermal wind is not able to describe the vertical variation of the temperature advection pattern. Quite frequently we find regions of cold air advection superimposed on warm air advection in the same vertical column and vice versa. The only way to incorporate such features is to introduce more information levels to get a better vertical resolution of the model.

From the operational point of view it is obvious that as few levels as possible are desirable. Not only does this decrease the time required to compute the forecasts, but the analysis problem becomes also less time consuming. One may therefore ask whether the addition of one extra information level will change the behavior of the model to such an extent that we can expect substantial differences between the three- and the two-parameter models.

It is the purpose of this study to show that the distributions of divergence and vertical velocity which are inherent in the three-parameter model show a great similarity to the distributions obtained by Charney [1], Fleagle [2] and more recently Hinkelmann [3]. A treatment of the three-parameter model as compared to the continuous case has the advantage that the solutions for divergence and vertical velocity considering relatively simple flow patterns can be expressed in such a form that the importance of the different factors contained in the solution can be easily investigated. We shall thus be able to consider the importance of the vertical variation of stability and the variation of wind speed with height, especially a crude measure of the curvature of the wind profile. Another advantage in this case is that we shall be able to study the solution for different horizontal scales.

The vertical variation of static stability will in this study be prescribed as a function of pressure in such a way that we obtain the major part of its systematic climatological variation. It should be stressed that this variation does not necessarily correspond to the synoptic variability.

It is necessary to restrict the investigation in this paper to flow patterns where the zonal wind is constant in each

581868—61——2

isobaric surface, but of course can vary with pressure, and to waves of the simple sinusoidal type. The results which can be obtained in this way are of course not directly applicable to the real atmosphere with its much more complicated flow pattern. Solutions for observed atmospheric flow patterns can be obtained by numerical methods. The diagnosis of the real atmosphere using equations very similar to those in this paper is presented by Cressman in another paper in this issue.

2. THE COMPUTATION OF VERTICAL VELOCITY IN THE THREE-PARAMETER CASE

The three-parameter representation of the atmosphere allows a solution for the vertical velocity at two internal levels in each vertical column in addition to the two values obtained from the boundary conditions at the top of the atmosphere and at the ground. Using a finite difference form of the continuity equation we can consequently obtain three values of the divergence at the intermediate levels. In this paper we shall for simplicity divide the atmosphere into six layers, each corresponding to $p_g/6$ cb., where p_g is the pressure at the ground (fig. 1). We shall assume that $p_g=100$ cb. and thus neglect the effect of topography. The boundary conditions for the vertical velocity, $\omega=dp/dt$, will be $\omega=0$ for $p=0$ and $p\equiv p_g$. It is quite likely that it will be an advantage to assume $\omega=0$ at some level in the stratosphere in the practical application and also to include the effects of the topography and friction at the lower boundary.

The equation for the vertical velocity is obtained from the vorticity equation in the form:

$$\frac{\partial\zeta}{\partial t}+\mathbf{V}\cdot\nabla(\zeta+f)=f_0\frac{\partial\omega}{\partial p} \tag{2.1}$$

and the adiabatic equation

$$\frac{\partial}{\partial t}\left(\frac{\partial\psi}{\partial p}\right)+\mathbf{V}\cdot\nabla\left(\frac{\partial\psi}{\partial p}\right)+\frac{\sigma}{f_0}\omega=0. \tag{2.2}$$

In (2.1) and (2.2) $\mathbf{V}=\mathbf{k}\times\nabla\psi$ is the horizontal wind assumed to be nondivergent, $\mathbf{k}$ a vertical unit vector, ψ the streamfunction, $\zeta=\nabla^2\psi$ the vertical component of the relative vorticity, f the Coriolis parameter, $\omega=dp/dt$ the vertical velocity, and $\sigma=-\alpha\partial\ln\theta/\partial p$ a measure of static stability; α is specific volume and θ potential temperature. The vertical derivative of the geopotential has been replaced by the vertical derivative of the streamfunction in the adiabatic equation (2.2) using the approximate relation (Phillips [5])

$$\partial\psi/\partial p=1/f_0\cdot\partial\phi/\partial p \tag{2.3}$$

where $\phi=gz$ is the geopotential, g the acceleration of gravity, and z the height of the isobaric surface.

From (2.1) and (2.2) we obtain the ω-equation

$$\sigma\nabla^2\omega+f_0^2\frac{\partial^2\omega}{\partial p^2}=f_0\left[\frac{\partial}{\partial p}(\mathbf{V}\cdot\nabla(\zeta+f))-\nabla^2\left(\mathbf{V}\cdot\nabla\frac{\partial\psi}{\partial p}\right)\right]. \tag{2.4}$$

In the derivation of (2.4) it has further been assumed that the horizontal variation of the static stability can be neglected, while a vertical variation is still possible.

The procedure to be followed is now to apply (2.4) at the levels 2 and 4 (see fig. 1), to approximate vertical derivatives by finite differences in a straightforward way, and in this way obtain two equations both containing ω_2 and ω_4 as unknowns. The streamfunction, ψ, has then to be known at the levels 1, 3, and 5. It is, however, convenient to introduce the new quantities

$$\left.\begin{aligned}\psi'&=\psi_1-\psi_3\\ \psi''&=\psi_3-\psi_5\end{aligned}\right\} \tag{2.5}$$

ψ' and ψ'' are the streamfunctions for the thermal flow in the layers between levels 1 and 3 and levels 3 and 5, respectively, and are of course measures of the mean temperatures in these layers.

Applying finite differences and using the boundary conditions for ω, we arrive after certain simple manipulations at the following set of equations for ω_2 and ω_4:

$$\left.\begin{aligned}\sigma_2\nabla^2\omega_2-\frac{2f_0^2}{P^2}\omega_2+\frac{f_0^2}{P^2}\omega_4&=\frac{f_0}{P}[\nabla^2(\mathbf{V}_3\cdot\nabla\psi')\\ &\quad-\mathbf{V}_3\cdot\nabla\zeta'-\mathbf{V}'\cdot\nabla\eta_3-\mathbf{V}'\cdot\nabla\zeta']\\ \sigma_4\nabla^2\omega_4-\frac{2f_0^2}{P^2}\omega_4+\frac{f_0^2}{P^2}\omega_2&=\frac{f_0}{P}[\nabla^2(\mathbf{V}_3\cdot\nabla\psi'')\\ &\quad-\mathbf{V}_3\cdot\nabla\zeta''-\mathbf{V}''\cdot\nabla\eta_3+\mathbf{V}''\cdot\nabla\zeta'']\end{aligned}\right\} \tag{2.6}$$

P is a constant pressure interval equal to 33⅓ cb. Equations (2.6) is the system which has to be solved for ω_2 and ω_4 given the three streamfunctions ψ_3, ψ', and ψ''.

The three streamfunctions will be prescribed by the expressions:

$$\left.\begin{aligned}\psi_3&=-U_3y+A_3\sin kx\\ \psi'&=-U'y+A'\sin(kx+\alpha')\\ \psi''&=-U''y+A''\sin(kx+\alpha'').\end{aligned}\right\} \tag{2.7}$$

U_3, U', and U'' are the zonal wind at level 3 and the thermal winds in the layers above and below this level. All three will be assumed to be constant. A_3, A', and A'' are the amplitudes of the streamfunctions. It is seen that kA_3, kA' and kA'' are the maximum meridional wind components in the three fields. α' and α'' measure the phase lag of the two thermal fields relative to the streamfunction at level 3. Positive values of the α's mean that the thermal field is lagging behind the stream field at level 3.

It is pertinent to mention that the values of α' and α'' determine the mean slope of the trough and ridge lines in the layers between the levels 1 and 3 and the levels 3 and 5, respectively. α' and α'' determine together a measure of the change in slope with height of the pressure systems.

The flow pattern at level 1 is obtained by adding the expressions for ψ_3 and ψ'. Applying simple trigonometric formulas we may write the streamfunction at level 1 in the form:

$$\psi_1=-(U_3+U')y+A_1\sin(kx+\gamma_1) \tag{2.8}$$

where

$$A_1=(A_3^2+A'^2+2A_3A'\cos\alpha')^{1/2} \tag{2.9}$$

and

$$\tan\gamma_1=\frac{A'\sin\alpha'}{A_3+A'\cos\alpha'}. \tag{2.10}$$

It is thus seen that γ_1 will be positive if $\alpha'>0$ provided α' is not so large that $A_3+A'\cos\alpha'<0$. In a similar way the flow pattern at level 5 can be written:

$$\psi_5=-(U_3-U'')y+A_5\sin(kx-\gamma_5) \tag{2.11}$$

where

$$A_5=(A_3^2+A''^2-2A_3A''\cos\alpha'')^{1/2} \tag{2.12}$$

and

$$\tan\gamma_5=\frac{A''\sin\alpha''}{A_3-A''\cos\alpha''}. \tag{2.13}$$

Again we find that γ_5 and α'' in general have the same sign for atmospheric flow patterns. We have thus seen that positive values of α' and α'' mean that the flow at level 1 is lagging behind the flow pattern at level 3, while the flow pattern at level 5 precedes that at level 3. Positive values of α' and α'' indicate therefore the usual westward tilt of the pressure systems, but the slope of a system is not necessarily linear in pressure.

When the expressions (2.7) are substituted in the right hand sides of equations (2.6) we get the following set of equations:

$$\left.\begin{aligned}\sigma_2\nabla^2\omega_2-\frac{2f_0^2}{P^2}\omega_2+\frac{f_0^2}{P^2}\omega_4&=\frac{f_0}{P}\,[2U'k^3A_3\cos kx\\&\qquad -kA'(\beta-U'k^2)\cos(kx+\alpha')]\\ \sigma_4\nabla^2\omega_4-\frac{2f_0^2}{P^2}\omega_4+\frac{f_0^2}{P^2}\omega_2&=\frac{f_0}{P}\,[2U''k^3A_3\cos kx\\&\qquad -kA''(\beta+U''k^2)\cos(kx+\alpha'')].\end{aligned}\right\} \tag{2.14}$$

The solutions to the system (2.14) will be of the form:

$$\left.\begin{aligned}\omega_2&=B_1\cos kx+B_2\cos(kx+\alpha')+B_3\cos(kx+\alpha'')\\ \omega_4&=C_1\cos kx+C_2\cos(kx+\alpha')+C_3\cos(kx+\alpha'').\end{aligned}\right\} \tag{2.15}$$

The amplitudes $B_{1,2,3}$ and $C_{1,2,3}$ can be determined by substitution of (2.15) into (2.14) and equating the coefficients of $\cos kx$, $\cos(kx+\alpha')$, and $\cos(kx+\alpha'')$. When this procedure is carried through we find the following expressions for the two vertical velocities:

$$\omega_2=\frac{1}{\Delta}\frac{f_0}{P}\left[-\left\{U'\left(\sigma_4k^2+\frac{2f_0^2}{P^2}\right)+U''\frac{f_0^2}{P^2}\right\}k^2v_3+\left(\sigma_4k^2+\frac{2f_0^2}{P^2}\right)(\beta-U'k^2)v'+\frac{f_0^2}{P^2}(\beta+U''k^2)v''\right] \tag{2.16}$$

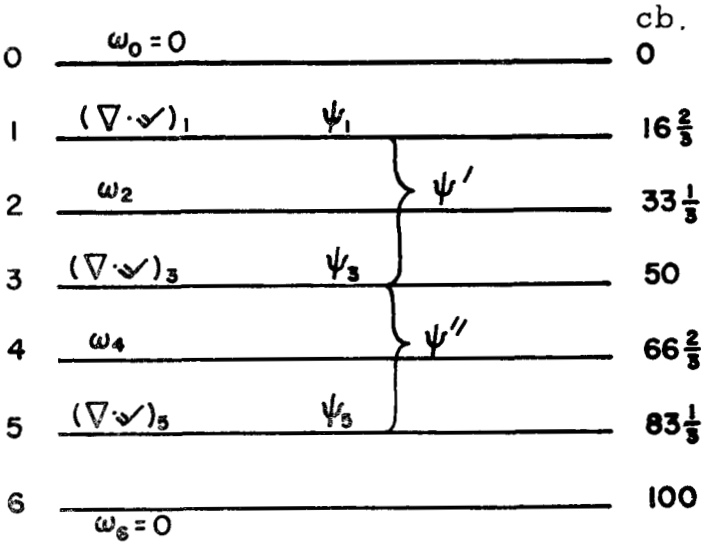

FIGURE 1.—Division of the atmosphere into six layers.

$$\omega_4=\frac{1}{\Delta}\frac{f_0}{P}\left[-\left\{U'\frac{f_0^2}{P^2}+U'''\left(\sigma_2k^2+\frac{2f_0^2}{P^2}\right)\right\}k^2v_3+\frac{f_0^2}{P^2}(\beta-U'k^2)v'+\left(\sigma_2k^2+\frac{2f_0^2}{P^2}\right)(\beta+U''k^2)v''\right]. \tag{2.17}$$

The quantity, Δ, appearing in (2.16) and (2.17) is a notation for the following expression

$$\Delta=\left(\sigma_2k^2+\frac{2f_0^2}{P^2}\right)\left(\sigma_4k^2+\frac{2f_0^2}{P^2}\right)-\left(\frac{f_0}{P}\right)^4. \tag{2.18}$$

The meridional components $v_3=kA_3\cos kx$, $v'=kA'\cos(kx+\alpha')$, and $v''=kA''\cos(kx+\alpha'')$ have also been introduced in the solutions (2.16) and (2.17).

From the knowledge of ω_2 and ω_4 obtained from (2.16) and (2.17) we can evaluate the divergence at the levels 1, 3, and 5, if we at the same time use the boundary conditions for ω; i.e., $\omega=0$ for $p=0$ and $p=p_g$.

The divergences are evaluated from the continuity equation in finite difference form. We get

$$(\nabla\cdot\mathbf{V})_1=-\frac{\omega_2}{P},\quad(\nabla\cdot\mathbf{V})_3=-\frac{\omega_4-\omega_2}{P},\quad(\nabla\cdot\mathbf{V})_5=\frac{\omega_4}{P} \tag{2.19}$$

3. DISCUSSION OF THE SOLUTION AND SOME EXAMPLES

To best illustrate the distribution of divergence and vertical motion zonal cross-sections are appropriate. To produce such cross-sections it is necessary to obtain values for the parameters, which are parts of the coefficients.

In the first example we have chosen a wavelength of 4000 km. The stability parameters, σ_2 and σ_4, were determined in such a way that they correspond to the usual increase of this parameter with height. It has been shown (Wiin-Nielsen [6]) that the variation of σ with pressure is described with good accuracy using the expression

TABLE 1.—*Values of U' and U''.*

Date, GMT	U', m.sec.$^{-1}$	U'', m.sec.$^{-1}$
Feb. 8, 1959, 1200	22.0	14.0
Feb. 10, 1959, 1200	21.4	12.6
Feb. 12, 1959, 1200	21.2	10.8
Feb. 16, 1959, 1200	17.2	9.8
Feb. 20, 1959, 1200	8.8	13.2
Mean	18.1	12.1

$$\sigma(p)=\sigma_3\left(\frac{50}{p}\right)^2 \tag{3.1}$$

where σ_3 is the value of the stability at 50 cb. The present operational model applies a value of σ_3 equal to approximately 3 MTS-units. Using (3.1), we get

$$\sigma_2\simeq 9 \text{ MTS-units}, \quad \sigma_4\simeq 2.25 \text{ MTS-units}. \tag{3.2}$$

The values of the thermal winds, U' and U'', were determined from actual wind data for a number of individual days. The mean zonal winds were available at the levels 85, 50, and 30 cb. U' and U'' were then obtained by linear extrapolation and interpolation. The values are given in table 1.

The mean values, $U'=18$ m.sec.$^{-1}$, $U''=12$ m.sec.$^{-1}$ were used in the examples. The striking feature for the five days in February 1959 is that the average shear is 50 percent larger in the upper layer than in the lower layer. It is interesting to see whether this result holds in general for the middle latitude in winter. From wind statistics for the period February 10, 1959 to April 10, 1959 it was found that the mean value of U' was 16 m.sec.$^{-1}$ and of U'' 9.5 m.sec.$^{-1}$ Data presented by Petterssen ([4], p. 98) for Larkhill covering a 2-year period gave the values $U'=14$ m.sec.$^{-1}$, $U''=7$ m.sec.$^{-1}$ It may therefore be safely concluded that the vertical shear of the horizontal wind is somewhat larger above than below 50 cb. in middle latitudes in winter. The maximum values of the meridional wind components were chosen to be: $v'=12$ m.sec.$^{-1}$, $v''=8$ m.sec.$^{-1}$, and $v_3=16$ m.sec.$^{-1}$

The last two parameters for which numerical values have to be chosen are α' and α''. In the first computation the values $\alpha'=10°$ and $\alpha''=20°$ were selected. These values correspond to $\gamma_1=4°$ and $\gamma_5=14°$ as computed from (2.10) and (2.13). As 360° corresponds to 4000 km. we find that the trough line at level 1 is only about 44 km. behind the trough line at level 3, while the trough line at the lower level (level 5) precedes the trough at level 3 by about 156 km. This first case has therefore a very small slope but a somewhat larger slope in the lower layer than in the upper. This difference in slope is characteristic for many atmospheric systems.

Figure 2 shows the distribution of the divergence in a zonal cross-section through a half wavelength. The heavy dashed line in the central part of the figure is the position of the trough line. The heavy solid line is the isoline for zero-divergence. We find in this case that the nondivergent level outside the trough region is situated a little above the 500-mb. surface. However, as we approach the trough line from the west the line for zero-divergence goes down to lower levels and intersects level 5 to the west of the trough position. Approaching the trough line from the east the zero-divergence line goes up and intersects with level 1 to the east of the trough at this level. We find therefore convergence at all levels in the trough. At the lower level we find convergence to the east of the trough and divergence to the west, while the opposite is the case at the higher level.

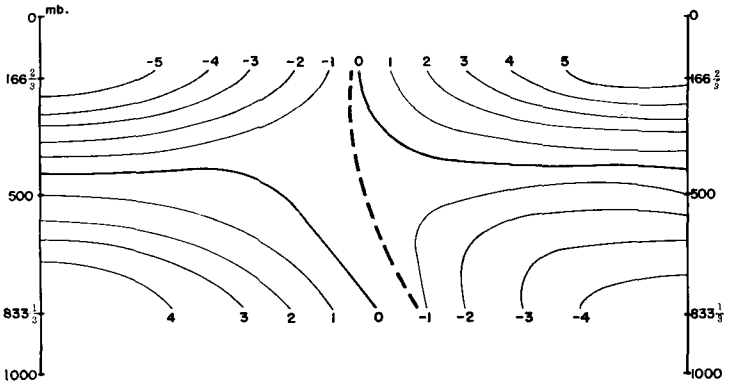

FIGURE 2.—Distribution of divergence in a zonal cross-section through a half wavelength. In this case the wavelength is 4000 km. and the stability parameters correspond to the usual increase of stability with height. West is to the left, east to the right. The heavy dashed line is the position of the trough line.

The distribution of divergence shown in figure 2 agrees to a very large extent with the distributions computed by Charney [1], Fleagle [2], and Hinkelmann [3]. It seems therefore that the major features of the distribution of divergence in a continuous model can be reproduced by a three-parameter model.

It was found of interest to investigate the distribution of divergence in the same zonal cross-section, if the vertical variation of the stability parameter was disregarded. In this computation it was assumed that $\sigma_2=\sigma_4=\sigma_3$ where σ_3 was set equal to a standard value. The resulting distribution of divergence is reproduced in figure 3. Comparing figure 2 with figure 3 one sees that the distributions are similar in a qualitative sense. The divergence pattern at level 3 has, however, an amplitude about 6 times larger in figure 3 than in figure 2, while the divergence is increased by a factor of 2 at level 1. It seems therefore important at least to incorporate an increase of the stability parameter σ with height in an operational model because the divergence and the vertical velocity are quite sensitive to this variation.

This fact is also illustrated in figure 4 which shows the distribution of the vertical velocity through a half wavelength at level 2. The solid line corresponds to the case where the vertical variation of stability is incorporated, while the dashed line is the distribution of the vertical

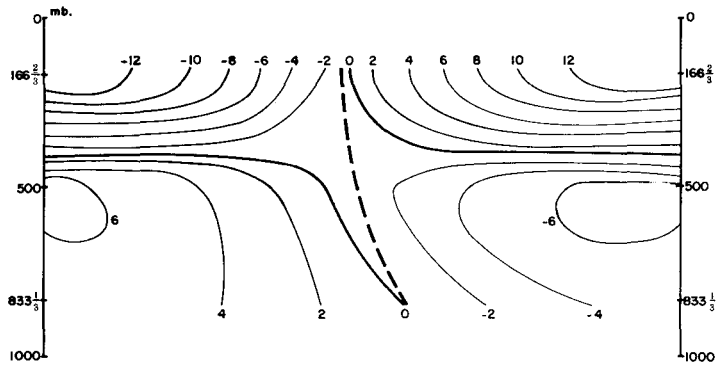

FIGURE 3.—Distribution of divergence in the same zonal cross-section as in figure 2. In this case the stability parameter is set to a standard value and does not vary in the vertical.

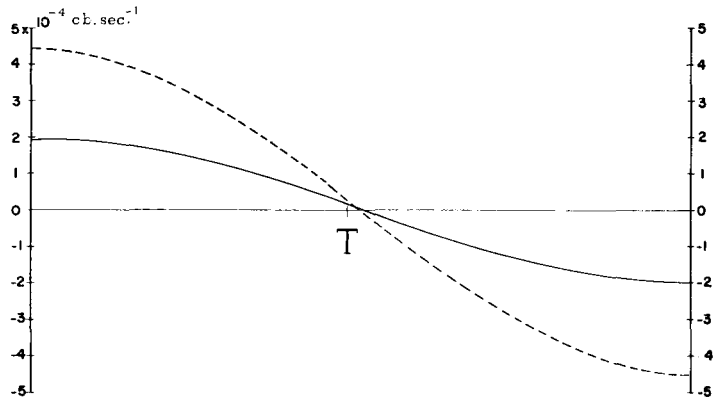

FIGURE 4.—Distribution of vertical velocity through a half wavelength at level 2 (33⅓ cb.). The solid line corresponds to the case with vertical variation of stability, the dashed line to the case of no vertical variation of stability. "T" designates position of the trough line.

velocity in the case where $\sigma_2=\sigma_4=\sigma_3$. The damping influence of the increase of the stability parameter, σ, is clearly seen in the figure. A similar figure (not reproduced) at the lower level (level 4) shows a very small difference between the corresponding curves. This is explained by the very small vertical variation of σ in the lowest layer of the troposphere.

4. ON SOME FACTORS INFLUENCING THE MID-TROPOSPHERIC DIVERGENCE

The divergence at level 3 estimated from the values of ω_2 and ω_4, which in turn are found by solving the two coupled ω-equations, will be used in a numerical prediction in the divergence term in the vorticity equation. It is therefore of importance to investigate the different factors which influence the distribution and magnitude of this divergence. In the present model with three information levels we have at least a first approximation to the curvature of the vertical profile of the zonal wind. We have further found in the preceding section that the vertical variation of the stability parameter is of importance for the magnitude of the mid-tropospheric divergence, but not so much for the distribution.

In order to simplify the first part of the discussion we shall for a moment neglect the vertical variation of the stability σ. With this simplification we obtain from (2.16) and (2.17)

$$(\nabla\cdot\mathbf{V})_3=\frac{f_0}{\sigma P^2+3f_0^2/k^2}\cdot[-2(U'-U''')v_3 -(U''-\beta/k^2)v'-(U'''+\beta/k^2)v'']. \quad (4.1)$$

The first term in the bracket of (4.1) represents the influence on the divergence patterns at level 3 caused by the crude measure of the curvature of the vertical profile of the horizontal wind. It is seen that $(U'-U'')$ is proportional to the second derivative of U with respect to pressure:

$$\frac{d^2U}{dp^2}\simeq\frac{1}{P^2}(U'-U'''). \quad (4.2)$$

If $U'>U''$ as in the example represented in figures 2 and 3 the first term will result in convergence where $v_3>0$, i.e. between the trough and the next ridge downstream, and divergence between the ridge and the following trough. The opposite distribution will result if $U'<U''$. The influence of the first term is therefore to increase the instantaneous speed of propagation of the wave if $U'>U''$, and to decrease the speed if $U'<U''$, but the term has no influence on the instantaneous deepening or filling.

In barotropic forecasts for 500 mb. it is often found that a trough is forecast to move too slowly in the southern portion, essentially in the region of the subtropical jet stream. According to synoptic investigations of the vertical wind profile in this wind system we find $U'>U''$. It is therefore possible that the contribution from the first term in (4.1) will help to remove this error.

Let us next turn our attention to the last two terms in (4.1). If the wavelength is so short that $(U'-\beta/k^2)$ is positive we find that both terms produce convergence where v' and v'' are positive and divergence where they are negative. If therefore the temperature patterns, ψ' and ψ'', are lagging behind the flow ψ_3, both of these terms contribute to produce convergence in the trough and thus give a tendency for deepening. However, for waves which are so long that $(U'-\beta/k^2)$ is negative, the second term changes sign and the two last terms counteract each other. In a qualitative way this argument shows that the shorter waves develop faster than the longer.

Equation (4.1) is somewhat simplified because we have assumed that $\sigma_2=\sigma_4$. If this assumption is removed we get a more complicated expression for the mid-tropospheric divergence. Subtracting (2.16) and (2.17) we obtain:

$$(\nabla \cdot \mathbf{V})_3 = \frac{f_0 k^2}{P^2 \Delta} [-\{U'(\sigma_4 k^2 + f_0^2/P^2) - U''(\sigma_2 k^2 + f_0^2/P^2)\} v_3$$
$$-(\sigma_4 k^2 + f_0^2/P^2)(U' - \beta/k^2) v'$$
$$-(\sigma_2 k^2 + f_0^2/P^2)(U'' + \beta/k^2) v'']. \quad (4.3)$$

The more general expression (4.3) shows that it is not only the difference in the vertical shear which counts in the first term in the bracket. The thermal wind U' in the upper layer is now multiplied by a factor depending on the stability in the lower layer, while U'' is multiplied by a factor containing the stability in the upper layer. Using standard values of σ_2 and σ_4 we can find the ratio $(U'/U'')_c$ which would give no contribution from the first term in the bracket of (4.3). The ratio $(U'/U'')_c$ is given as a function of wavelength in table 2 computed from the formula:

$$\left(\frac{U'}{U''}\right)_c = \frac{\sigma_2 k^2 + f_0^2/P^2}{\sigma_4 k^2 + f_0^2/P^2}. \quad (4.4)$$

From the table it is seen that the vertical variation of stability has the greatest influence on the divergence for the shorter waves. With no variation of the stability we get convergence ahead of the trough if only $(U' - U'')$ is positive. The values in table 2 show that U' would have to be at least two times larger than U'' to get the same sign of the divergence for a wave with a wavelength of 4000 km. The table shows also that only a minor modification is introduced for the very long waves as compared to the results derived from the simplified formula (4.1). For a given value of (U'/U'') characteristic of atmospheric conditions, say 1.5, the first term in (4.3) would result in divergence ahead of the trough in short waves, but convergence in the same region for long waves.

With respect to the last two terms in (4.3) we find some modification of the magnitude, but no change of the sign. The contributions from the terms are, however, large enough to give convergence to the east of the trough line in figure 2 as well as in figure 3.

Figure 5 shows the distribution of convergence and divergence in a zonal cross-section in a more extreme case. The distribution shown in figure 5 was computed using the same parameters as in figure 2 except that the phase differences between the temperature fields and the stream function at 500 mb. were larger in the case illustrated by figure 5. In the construction of figure 5 it was assumed that $\alpha' = 45°$ and $\alpha'' = 90°$, which means that the temperature field in the upper layer lags ⅛ of a wavelength behind the streamfunction at 500 mb., while the lag in the lower layer is ¼ of a wavelength. The result of the assumption is a larger slope of the trough line. From the formulas (2.10) and (2.13) it follows that the trough at level 5 precedes the 500-mb. trough by about 300 km., while the trough at level 1 lags about 210 km. behind the 500-mb. trough.

TABLE 2.—*Values of* $(U'/U'')_c$ *as a function of wavelength.*

$L \times 10^{-3}$ km.	1	2	3	4	5	6	7	8	10	12	14	28
$(U'/U'')_c$	3.6	3.0	2.4	2.0	1.7	1.5	1.4	1.3	1.2	1.2	1.1	1.0

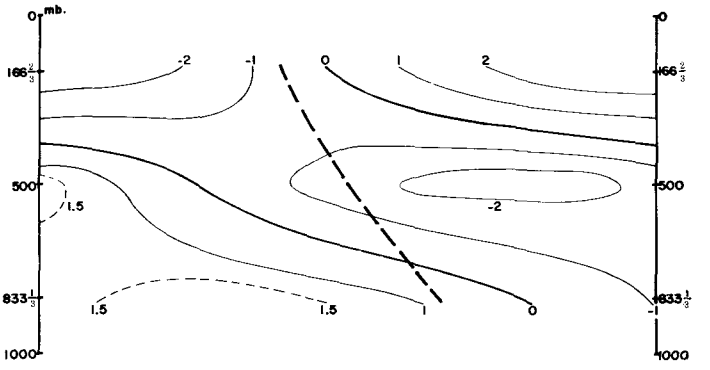

FIGURE 5.—Distribution of divergence in the same zonal cross-section as in figure 2. In this case the phase differences between the temperature fields and streamfunction at 500 mb. were larger than in case shown in figure 2.

The main effect of the greater vertical tilt of the system is, as seen from figure 5, to produce a larger slope of the convergence pattern. The convergence in and ahead of the trough line has now a maximum in the midtroposphere amounting to about 2×10^{-6} sec.$^{-1}$ with divergence above and below.

5. REMARKS ON THE DIVERGENCE IN VERY LONG WAVES

Due to the special difficulties encountered in forecasting the very long waves in the atmosphere it is of interest to investigate the distribution of divergence in such waves in the present model. It is apparent from (4.3) that the terms containing the vertical stability become of minor importance when the wave number is small. In the same case it is seen that the two β-terms become dominating in the last two terms of the bracket in (4.3). These two β-terms appear, however, with opposite sign and therefore tend to compensate if v' and v'' are of the same order of magnitude and in phase. The importance of the first term for the determination of the divergence distribution in this model is the difference, $(U' - U'')$. As we find that $(U' - U'')$ is positive in the jet stream regions where the waves have the greatest amplitude, the contribution is to produce convergence to the east of the trough and divergence to the west in the very long waves and thus obtain a decrease of the retrogression. Forecast experiments with the model will show whether the magnitude of the divergence is large enough to control the very long waves.

We may estimate the divergence from (4.3). Assuming the same values of the stability as in figure 3 ($\sigma_2=9$ and $\sigma_4=2.25$ MTS-units) and further $U'=18$ m.sec.$^{-1}$, $U''=12$ m.sec.$^{-1}$ we find in middle latitudes ($f_0=10^{-4}$ sec.$^{-1}$) for $k^2=0.2\times10^{-12}$m.$^{-2}$, corresponding to two waves around the hemisphere:

$$(\nabla\cdot\mathbf{V})_3=-[0.29\ v_3-3.78\ v'+6.29\ v'']\times10^{-8}\ \text{sec.}^{-1} \quad (5.1)$$

Assuming further that the waves v_3, v', and v'' are in phase and adopting the values $v_{3,\max}=16$ m.sec.$^{-1}$, $v'_{\max}=12$ m.sec.$^{-1}$, and $v''_{\max}=8$ m.sec.$^{-1}$ we find that

$$(\nabla\cdot\mathbf{V})_3\cong-10^{-7}\cos kx \quad (5.2)$$

if the streamfunction at level 3 is

$$\psi_3=-U_3\ y+A_3\sin kx. \quad (5.3)$$

We find therefore in this case a distribution of divergence which would counteract the retrogression of the very long waves.

6. SUMMARY AND CONCLUSIONS

The distribution of vertical velocity and divergence in a three-parameter model of the atmosphere has been investigated. Section 2 contains the formulation of the problem and the formal solution of the equation for the vertical velocity in the model for simple sinusoidal waves. The solution obtained in section 2 is discussed in the next section, where the importance of the vertical variation of static stability and the vertical profile of the horizontal wind is pointed out. Examples showing the distribution of divergence in zonal cross-sections are shown. It is found that the distribution of divergence in the three-level model to a large extent resembles distributions by others with more complicated models.

The different factors influencing the mid-tropospheric divergence are investigated in section 4. It is found that the vertical profile of the wind is most important for the speed of propagation of the waves, while the vertical slope of the waves contributes to the development.

The last section contains a discussion of the distribution of divergence in very long waves and an example is computed.

REFERENCES

1. J. G. Charney, "The Dynamics of Long Waves in a Baroclinic Westerly Current," *Journal of Meteorology*, vol. 4, No. 5, Oct. 1947, pp. 135–162.
2. R. G. Fleagle, "Quantitative Analysis of Factors Influencing Pressure Change," *Journal of Meteorology*, vol. 5, No. 6, Dec. 1948, pp. 281–292.
3. K. Hinkelmann, "Ein Numerisches Experiment mit den primitiven Gleichungen," pp. 486–500 of *The Atmosphere and the Sea in Motion* (Rossby Memorial Volume), Rockefeller Institute Press, in association with Oxford University Press, New York, 1959, 509 pp.
4. S. Petterssen, *Weather Analysis and Forecasting*, vol. 1 "Motion and Motion Systems," McGraw-Hill Book Co. Inc., New York, 1956.
5. N. A. Phillips, "Geostrophic Errors in Predicting the Appalachian Storm of November 1950," *Geophysica*, vol. 6, No. 3–4, 1958, pp. 389–405.
6. A. Wiin-Nielsen, "On Barotropic and Baroclinic Models, with Special Emphasis on Ultra-Long Waves," *Monthly Weather Review*, vol. 87, No. 5, May 1959, pp. 171–183.